Paper No. 12

GROUND VIBRATION TEST

A TOOL FOR ROTORCRAFT DYNAMIC AND AEROELASTIC INVESTIGATIONS

by

F. Kießling

DFVLR - Institute for Aeroelasticity

Göttingen, Germany

Notation

Coordinate Systems

X, Y, Z	inertial coordinates
x, y, z	blade coordinates

Scalars

$\mathcal{D}$	dissipation function
D_{rr}	generalized damping
F_X, F_Y, F_Z	hub forces
I_X, I_Y, I_Z	rotor moments of inertia
K_{rr}	generalized stiffness
M	rotor mass
M_X, M_Y, M_Z	hub moments
$M_{r(r)}$	generalized mass
N	number of blades
$\mathcal{T}$	kinetic energy
$\mathcal{U}$	elastic potential energy
$\mathcal{W}$	work
f	frequency
k_A	radius of gyration of tension carrying cross-section around elastic axis
m	mass
n	number of degrees of freedom
q	generalized coordinate
t	time
u, v, w	displacements
δ	variation
ζ	damping coefficient
ϑ	pitch angle
θ	torsion angle
φ	rotation angle
ψ	azimuth angle
ω_r	circular eigenfrequency
Δ	phase resonance criterion
Ω	circular frequency of rotor revolution

Matrices

D	damping matrix
E	skew-symmetric matrix due to damping
F	applied forces
G	gyroscopic matrix
K	stiffness matrix
M	mass matrix
Q	generalized forces
R	inertial coordinates
T	transformation matrix
U	modal matrix
Φ	rotation matrix
Ψ	rotor rotation matrix
p, q	generalized coordinates
r	blade coordinates
$\mathbf{u}_r$	modal column

Superscripts

A, B	cyclic coordinates
C	collective coordinate
D	differential coordinate
T	transposed
a, b	cyclic mode shapes
c	collective mode shape
d	differential mode shape
α, β	cyclic (rotor-fixed) coordinates

Subscripts

A	tension axis
C	centrifugal
E	elastic
F	airframe
G	geometric
H	hub

L	linear	| |	modulus
Q	quadratic	$\mathcal{R}e$, $\mathcal{I}m$	real-, imaginary part
R	rotor	'	derivative with respect to x
e	elastic	·	derivative with respect to t
k	blade index	^	elastic axis
r, s	mode indices	⌜⌟	diagonal matrix
0	rigid-body		

Symbols

-	rotor-fixed system

1. Introduction

The development of advanced VTOL-configurations like tilt-rotor or stop-rotor aircraft poses severe dynamic and aeroelastic problems. To avoid troubles with ground- or air-resonance or with whirl flutter, for example, proper calculations must be carried out as soon as possible. Besides the formidable task to determine reasonable unsteady airloads induced by deformations of a rotorcraft, which is not considered here, it is obviously important to know the essential elastomechanical behaviour of the structure.

Helicopters suffer from forced vibrations due to the unsymmetrical flow conditions. There are attempts to reduce the vibration level or at least the significant peaks by means of active or passive isolation. Similar to stability investigations an adaequate dynamic representation of the whole system must be established for layout.

In practise, the mathematical model used for vibration problems is limited to a finite number of degrees of freedom. Although thousands of them can be handled nowadays in connexion with finite element techniques on large computers, there is a strong desire to put dynamic problems in a condensed form. Usually a normal mode approach is chosen for this purpose.

In the early stages of development the analyst must rely on his skill of establishing an appropriate mathematical model. As soon as the prototype or at least some essential hardware components become available, an experimental determination of dynamic characteristics in terms of normal modes and their associated parameters can be undertaken by a ground vibration test. It is common practise in the fixed-wing community to use the results for ultimate flutter calculations or at least to check and improve the finite element model. Continuous improvements of the measurement techniques have broadened the scope of ground vibration tests. For example, dynamic response calculations for spacecraft structures are often supported by a modal survey test.

2. General Remarks on Ground Vibration Testing

Before proceeding to special problems of rotary wings, some remarks on modern ground vibration test techniques seem to be opportune. A lot of proposals has been published in recent years, for example refs. [1], [2], showing alternatives to the "classical" phase-resonance procedure. Without attempting an appraisal of various new methods this paper features an improved phase-reso-

nance approach used by the DFVLR-Institute for Aeroelasticity in a series of tests on airplanes and satellite structures, [3].

2.1 Test Objectives

The mathematical model describing small motions of a linear elastic and lightly damped structure can be written with a set of n generalized coordinates $\mathbf{q}$ corresponding to normal modes $\mathbf{u}$

$$\mathbf{M}\ddot{\mathbf{q}} + \mathbf{D}\dot{\mathbf{q}} + \mathbf{K}\mathbf{q} = \mathbf{Q} \tag{1}$$

A viscous type of damping is assumed for convenience. The generalized forces are

$$\mathbf{Q} = \mathbf{U}^T \mathbf{F} \tag{2}$$

where applied forces (and moments) are contained in $\mathbf{F}$. Because of the orthogonality property of normal modes, the generalized mass matrix $\mathbf{M}$ and the generalized stiffness matrix $\mathbf{K}$ are diagonal and for the elements

$$K_{rr} = \omega_r^2 M_{rr}, \qquad r = 1, 2, \ldots, n \tag{3}$$

holds. From a physical point of view, there is no indication that the generalized damping matrix has to be diagonal, too. Faced with uncertainties of damping determination it is usual to assume a diagonal form facilitating computational work. A modal damping coefficient ζ is defined by

$$D_{rr} = 2\zeta_r \omega_r M_{rr}, \quad r = 1, 2, \ldots, n \tag{4}$$

The test objectives of a ground vibration test can now clearly be seen. The mathematical model requires

- eigenfrequencies ω_r
- normal mode shapes $\mathbf{u}_r \qquad r = 1, 2, \ldots, n$
- generalized masses $M_{r(r)}$
- damping matrix $\mathbf{D}$ or
- damping coefficients ζ_r

taking proper support conditions into account. In the case of aircraft, it is advisable to simulate the unconstrained state by means of a soft suspension system. The set of orthogonal rigid-body modes (zero eigenfrequency and damping) can be included consistently in eq.(1).

2.2 Test Method

The quantities above can be obtained by application of the phase-resonance principle:

> Having tuned the frequency and the distribution of in- or anti-phase sinusoidal excitation forces at a resonance in such a way that displacements of all points are in quadrature, the structure vibrates at an eigenfrequency and the response is the corresponding normal mode of the undamped system.

It can be imagined that in case of complex structures this condition will not be met easily. Firstly, all resonances must be identified by sweep tests, for example. Then the isolation of a normal mode requires an individual adjustment of the forces which must be set by trial and error while monitoring many response sig-

nals. The proper excitation can be prevented by inaccessibility of the structure. Together with frequency clusters and damping coupling this makes it difficult to get a pure mode. Furthermore, experience has shown, that real structures behave sometimes clearly non-linear. This is especially true when controls of an aircraft are considered. In the future substantial efforts must be undertaken towards proper handling of non-linearities and their effect on test methods based on linear models.

Generalized masses are determined experimentally by frequency shifting methods, for example. Small shifts of an eigenfrequency are produced by additional masses or springs and by additional forces in quadrature. Damping values can be obtained by measuring the input energy. A simple alternate method consists in switching-off the excitation and recording the decay of several points. This procedure is limited in practise to well-separated modes.

2.3 Test Procedure

A schematic test set-up with the facilities of the DFVLR-Institute for Aeroelasticity is shown in Figure 1. A frequency generator provides the reference signal for power amplifiers, which supply up to 10 electrodynamic exciters. Frequency and force distribution can be controlled individually. The response is measured by up to 300 accelerometers. Their signals are amplified and separated into real and imaginary parts. These values are digitized and fed to a process computer, which performs calculation of generalized masses and output of modal data. During identification and isolation phases of the test a "Phase-Resonance-Criterion"

$$\Delta = \frac{\sum_{\nu=1}^{\mu} |\ddot{u}_\nu| \cdot \mathcal{R}e(\ddot{u}_\nu)}{\sum_{\nu=1}^{\mu} |\ddot{u}_\nu|^2} \tag{5}$$

is computed "on-line" with μ complex acceleration signals ν . It is zero (minimum), if the phase-resonance condition is exactly (approximately) satisfied. This single value is independent of amplitude and makes it easy to find an optimum excitation.

3. The Special Case of Rotorcraft

Structures with rotating parts require more subtle considerations. It is a well-known procedure to take into account the effect of running rigid propellers by means of a skew-symmetric gyroscopic matrix,[4]. This results in complex modes and real eigenfrequencies of the undamped system. But even in the case of hingeless types, helicopter rotors are far from being rigid and careful attention has to be given to this fact. Large steady-state tension stresses produced by rapid spin of the rotor do work with second-order strains resulting in a "geometric" stiffness matrix. The centrifugal body forces give rise to additional stiffness terms. The gyroscopic matrix is extended due to elastic blade motions.

Sometimes it may be essential to retain non-linear inertial terms in the equations of motion. Nevertheless, the mathematical model adopted in this context is a linear one, simply to permit a modal approach and the principle of superposition.

3.1 Test Configurations

At a glance it seems attractive to perform the test on the whole craft with spinning rotor, because all effects mentioned above are included. But there are important objections against this approach. Intending to get elastomechanical parameters, the aerodynamic forces acting on the blades will introduce error. Strictly speaking, such a test has to be carried out in a vacuum chamber and this is practicable for models only. The "noisy" environment can disturb the measurement considerably and the transmission of signals from a rotating to a stationary system presents some problems. The phase-resonance method will fail, because an appropriate excitation of the rotating blades is generally not possible and the phase criterion becomes meaningless in the presence of complex natural modes.

At least for practical reasons it is worthwile to look for methods based on tests with the rotor at rest. Then it must be accepted, that effects of spin are introduced by calculated corrections using test data. A three- or more-bladed rotor possesses - when perfectly constructed - certain symmetry properties. Advantage can be taken by them testing rotor and airframe separately. The latter can be investigated in a standard manner. Mounting a rigid mass dummy in place of the rotor will reduce the frequency range to be explored in this test.

Recently, C. T. TRAN, W. TWOMEY, and R. DAT published a method, which uses the normal modes of a single blade fixed at a wall, [5]. It can be difficult to realize the boundary conditions existing at the actual rotor hub. Therefore, in the following the unconstrained rotor is considered on the whole. In [6] the author has proposed to excite complex modes with phase angles equal to multiples of the angle between neighboured blades. Thereby all blades will execute the same motion. Typical mode shapes are shown in Figure 2. In practise, identical blades cannot be produced and even slight unsymmetries make it difficult to excite complex cyclic modes. For this reason the corresponding "antisymmetric" pairs of normal modes are chosen and by this way the necessity to deal with complex modes is removed, too.

3.2 Rotor Equations of Motion

The additional terms introduced by spin require an excursion to the mathematical model of a flexible rotor as illustrated in Figure 3. Four blades are especially chosen in this context. The Lagrange formalism is used to establish a set of linear differential equations

$$\frac{d}{dt}\left(\frac{\partial \mathcal{T}}{\partial \dot{\mathbf{q}}_R}\right) - \frac{\partial \mathcal{T}}{\partial \mathbf{q}_R} + \frac{\partial \mathcal{U}}{\partial \mathbf{q}_R} + \frac{\partial \mathcal{D}}{\partial \dot{\mathbf{q}}_R} = \mathbf{Q}_R \tag{6}$$

with kinetic energy $\mathcal{T}$, elastic potential energy $\mathcal{U}$, and dissipation function $\mathcal{D}$ of the unconstrained rotor. The generalized coordinates $\mathbf{q}_R$ can be partitioned into

$$\mathbf{q}_0 = \left[u_0\ v_0\ w_0\ \varphi_x\ \varphi_y\ \varphi_z\right]^T \tag{7}$$

describing rigid-body motions and $\mathbf{q}_e$ representing elastic motions, respectively. The generalized forces $\mathbf{Q}_R$ can be deduced from virtual work

$$\delta \mathcal{W} = \mathbf{Q}_R^T \delta\, \mathbf{q}_R \tag{8}$$

and will be zero when no hub and aerodynamic forces are considered. Performing integration and summation over all blades the kinetic energy reads

$$\mathcal{T} = \frac{1}{2} \sum_k \int \dot{\mathbf{R}}_k^T\, \dot{\mathbf{R}}_k\, dm \quad . \tag{9}$$

The time derivative of the column matrix

$$\mathbf{R}_k = \mathbf{R}_0 + \mathbf{\Phi}_x \mathbf{\Phi}_y \mathbf{\Phi}_z \mathbf{\Psi}_k \mathbf{r}_k \tag{10}$$

of inertial coordinates X_k, Y_k, Z_k of a mass element dm on blade k is needed. $\mathbf{R}_0$ containes the displacements u_0, v_0, w_0 of the rotor centre of mass. $\mathbf{\Phi}_x, \mathbf{\Phi}_y, \mathbf{\Phi}_z$ describe rotations of the reference frame, for example

$$\mathbf{\Phi}_x = \begin{bmatrix} 1 & 0 & 0 \\ 0 & \cos\varphi_x & -\sin\varphi_x \\ 0 & \sin\varphi_x & \cos\varphi_x \end{bmatrix} . \tag{11}$$

The position of the k-th blade is defined by

$$\mathbf{\Psi}_k = \begin{bmatrix} \cos\psi_k & -\sin\psi_k & 0 \\ \sin\psi_k & \cos\psi_k & 0 \\ 0 & 0 & 1 \end{bmatrix} , \tag{12}$$

where

$$\psi_k = \Omega t + \bar{\psi}_k \tag{13}$$

$$\bar{\psi}_k = \frac{2\pi}{N}(k-1) . \tag{14}$$

The coordinates of dm in the blade system, (x_k, y_k, z_k), can be split up into constant terms (x, y, z) and those depending in linear $(u, v, w)_k$ or quadratic $(u_Q, v_Q, w_Q)_k$ manner on the generalized coordinates $\mathbf{q}_e$, briefly written

$$\mathbf{r}_k = \mathbf{r} + \mathbf{r}_{Lk} + \mathbf{r}_{Qk} . \tag{15}$$

Performing rather tedious operations the kinetic energy expression with all terms up to second order will be obtained. The displacements u, v, w can be expressed by normal modes of the rotor at rest like

$$\bar{u}_k = \sum_r u_r^c q_r^C + \sum_r (u_r^a \cos\bar{\psi}_k - u_r^b \sin\bar{\psi}_k) q_r^\alpha + \sum_r (u_r^b \cos\bar{\psi}_k + u_r^a \sin\bar{\psi}_k) q_r^\beta + (-1)^k \sum_r u_r^d q_r^D \tag{16}$$

and by the transformation

$$\begin{bmatrix} q_r^\alpha \\ q_r^\beta \end{bmatrix} = \begin{bmatrix} \cos\Omega t & \sin\Omega t \\ -\sin\Omega t & \cos\Omega t \end{bmatrix} \begin{bmatrix} q_r^A \\ q_r^B \end{bmatrix} \tag{17}$$

$$u_k = \sum_r u_r^c q_r^C + \sum_r (u_r^a \cos\psi_k - u_r^b \sin\psi_k) q_r^A + \sum_r (u_r^b \cos\psi_k + u_r^a \sin\psi_k) q_r^B + (-1)^k \sum_r u_r^d q_r^D \tag{18}$$

is obtained. The so-called "multi-blade coordinates", [7], are grouped as indicated in Figure 2. The mode shapes u_r^a and u_r^b can be found by

(19) $$u_r^a = \frac{2}{N}\sum_k \bar{u}_{kr}\cos\bar{\psi}_k \quad \text{and} \quad u_r^b = -\frac{2}{N}\sum_k \bar{u}_{kr}\sin\bar{\psi}_k$$

from the shape of the "antisymmetric" normal mode q_r^α, for example. By use of eq. (18) the trigonometric terms are removed from $\mathcal{T}$ when summing up over k. Elastic potential energy and dissipation function of the rotor at rest can be expressed by

(20) $$\bar{\mathcal{U}} = \frac{1}{2}\left[\sum_r \omega_r^{C\,2} M_{rr}^C q_r^{C\,2} + \sum_r \omega_r^{\alpha\,2} M_{rr}^\alpha (q_r^{\alpha\,2} + q_r^{\beta\,2}) + \sum_r \omega_r^D M_{rr}^D q_r^{D\,2}\right]$$

and

(21) $$\bar{\mathcal{D}} = \left[\sum_r \zeta_r^C \omega_r^C M_{rr}^C \dot{q}_r^{C\,2} + \sum_r \zeta_r^\alpha \omega_r^\alpha M_{rr}^\alpha (\dot{q}_r^{\alpha\,2} + \dot{q}_r^{\beta\,2}) + \sum_r \zeta_r^D \omega_r^D M_{rr}^D \dot{q}_r^{D\,2}\right].$$

The transformation (17) must be applied to get $\mathcal{U}$ and $\mathcal{D}$. Performing the operations in eq. (6)

(22) $$\mathbf{M}_R \ddot{\mathbf{q}}_R + (\mathbf{G}_R + \mathbf{D}_R)\dot{\mathbf{q}}_R + (\mathbf{K}_R + \mathbf{E}_R)\mathbf{q}_R = \mathbf{Q}_R$$

is obtained. The symmetric $\mathbf{D}_R$ and the antisymmetric $\mathbf{E}_R$ matrix are caused by damping. The structure and coefficients of the various matrices are given in the appendix. The stiffness matrix is split up as follows:

(23) $$\mathbf{K}_R = \mathbf{K}_G + \mathbf{K}_C + \mathbf{K}_E .$$

By the special choice of rotor modes several orthogonality conditions permit considerable simplifications. So a diagonal mass matrix is obtained, for example.

Up to this point no special mathematical blade model has been adopted. To evaluate the matrix coefficients, which are not obtained by test, displacement functions may be defined in the following manner

$$u = -y\hat{v}' - z\hat{w}' + \int_0^x (y_A \hat{v}'' + z_A \hat{w}'' - k_A^2 \theta' \theta')\, dx$$

(24) $$v = \hat{v} - z\theta$$

$$w = \hat{w} + y\theta$$

and

$$u_Q = z\theta\hat{v}' - y\theta\hat{w}' + \int_0^x (y_A \theta \hat{w}'' - z_A \theta \hat{v}'' - \frac{\hat{v}'^2}{2} - \frac{\hat{w}'^2}{2} - k_A^2 \frac{\theta'^2}{2})\, dx$$

(25) $$v_Q = -\frac{y}{2}\theta^2$$

$$w_Q = -\frac{z}{2}\theta^2$$

where a separation of the mode shapes into flapping $\hat{w}$ and lagging $\hat{v}$ of the elastic axis and rotation θ has to be performed. The expressions contain the same approximations as used in reference [8]. In (5) the underscored terms are retained. Details of the complete approach above must be left to a forthcoming report.

3.3 Modal Synthesis

It remains the task to couple rotor and airframe. Using the results of a ground vibration test on the unconstrained airframe (rigid-body modes included) and on the unconstrained isolated rotor, the equations of motion with interaction forces and moments at the hub read

$$(26)\quad \begin{bmatrix} M_F & 0 & 0 \\ 0 & M_0 & 0 \\ 0 & 0 & M_e \end{bmatrix} \begin{bmatrix} \ddot{q}_F \\ \ddot{q}_0 \\ \ddot{q}_e \end{bmatrix} + \begin{bmatrix} 0 & 0 & 0 \\ 0 & G_{00} & G_{0e} \\ 0 & G_{e0} & G_{ee} \end{bmatrix} \begin{bmatrix} \dot{q}_F \\ \dot{q}_0 \\ \dot{q}_e \end{bmatrix} + \begin{bmatrix} K_F & 0 & 0 \\ 0 & 0 & 0 \\ 0 & 0 & K_e \end{bmatrix} \begin{bmatrix} q_F \\ q_0 \\ q_e \end{bmatrix} = \begin{bmatrix} U_{FH}^T & 0 \\ 0 & 1 \\ 0 & U_{eH}^T \end{bmatrix} \begin{bmatrix} F_{FH} \\ F_{RH} \end{bmatrix}$$

Damping and the other generalized forces are not included for brevity. From compatibility conditions

$$(27)\quad U_{FH}\, q_F = q_0 + U_{eH}\, q_e$$

a transformation

$$(28)\quad \begin{bmatrix} q_F \\ q_0 \\ q_e \end{bmatrix} = \begin{bmatrix} 1 & 0 \\ U_{FH} & -U_{eH} \\ 0 & 1 \end{bmatrix} \begin{bmatrix} q_F \\ q_e \end{bmatrix} = T\, p$$

is found, which reduces the size of the problem by six. Restoring symmetry, the equations of motion of the coupled system read

$$(29)\quad M\ddot{p} + G\dot{p} + K p = 0$$

There is a true zero column on the right side because of the equilibrium condition

$$(30)\quad F_{FH} + F_{RH} = 0$$

Eq. (29) may be subject to an eigenvalue/eigenvector analysis.

4. Application to a Simple Model

To illustrate the theoretical considerations about an unconstrained isolated rotor, a ground vibration test has been carried out on a simple model. In order to get some indication about measuring accuracy the test object was chosen in such a way to permit an exact analytical solution. The model consists of two homogeneous brass rods with rectangular cross section. They are clamped together at a massive hub forming a four-bladed "rotor" of 2 m diameter.

4.1 Test Set-up

The test arrangement is shown in Figure 4. The rotor has been suspended softly by rubber cords. By this way the rigid-body frequencies are placed below 2 cps . The details of the hub are shown in Figure 5. The test object was equipped with 48 pick-ups to measure in flap and lag directions. For excitation special non-contact electrodynamic exciters were used as shown in Figure 6. Elastic torsional deformations have not been taken into account, because the torsion eigenfrequency had been expected at 235 cps . This is considerably above the range to be investigated. The test was performed in not very elaborate manner. Generalized masses were determined by the additional mass procedure. Damping co-

efficients were obtained by the in-put energy method and for the lower modes by decay records, too.

4.2 Test Results

In Figure 7 the second antisymmetric flap bending of blade 2 and 4 is shown as an example for a mode obtained by test. Agreement with the analytical solution is good. Examining the complete test results the measurement of mode shapes shows a random error of 3 percent. The eigenfrequencies, generalized masses, and damping coefficients of all measured modes are listed in Table 1. Correlation with analytical results is generally good for eigenfrequencies but sometimes poor for generalized masses. The differences in antisymmetric modes can be attributed partly to the hub construction (the blades are not exactly arranged in a plane), which permits coupling between flap and lag motions. The blade offset was not considered in the analysis.

The determination of geometric stiffness terms requires products of derivatives of measured modes. This seems to be a critical point. Table 2 shows eigenfrequencies of differential modes, when the rotor is spinning at multiples of the first nonrotating flap bending frequency. The analytical values are based on an expansion using 6 nonrotating exact normal modes in flapping and lagging, respectively. The test values are obtained by using the measured modal parameters, of course, and by calculating geometric stiffness with aid of interpolating spline functions. Good correlation can be observed and this holds also for the mode shapes not listed here. By the use of three flap and two lag modes the truncation error in the normal mode approach is less than measuring accuracy.

5. Conclusions

Ground vibration tests on rotorcraft can be used to determine the elastomechanical parameters necessary for aeroelastic and dynamic analyses. After some general remarks the specific problems associated with rotor spin are discussed. Practically, full-scale tests are feasible on non-rotating components only. A method is presented, which uses the normal modes of the airframe together with those of the whole unconstrained rotor at rest. Compared with single blade testing this approach results in a reduction of coupling terms in the linear rotor equations of motion and has the advantage of better representation of blade root conditions by use of the actual hub. The effects of rotor spin are introduced by correction terms, which can be calculated with test data. Multiblade coordinates yield matrices with constant coefficients. Rotor and airframe are coupled by a modal synthesis.

A test on a simple four-bladed model generally shows good correlation with analytical results. The experimental determination of generalized masses involves larger errors and must be subject of further improvement.

The model test of the non-rotating isolated rotor described in this paper must be considered as a first step to an experimental substantiation of the whole approach. Further tests should deal with truncation errors introduced by modal synthesis, for example. A test on an idealized model with rotating rotor is intended using ground vibration test techniques with non-appropriate excitation. The results will be compared with those obtained by the proposed method.

6. References

1. H.G. Küssner, Theorie dreier Verfahren zur Bestimmung der Parameter eines elastomechanischen Systems. Z. Flugwiss. 19, 53-61 (1971).
2. H. Wittmeyer, Ein iteratives, experimentell-rechnerisches Verfahren zur Bestimmung der dynamischen Kenngrößen eines schwach gedämpften elastischen Körpers. Z. Flugwiss. 19, 229-241 (1971).
3. E. Breitbach, Neuere Entwicklungen auf dem Gebiet des Standschwingungsversuchs an Luft- und Raumfahrtkonstruktionen. VDI-Berichte 221, 33-40 (1974).
4. H. Försching, Dynamic aeroelastic calculations of aircraft based on ground-vibration test data. Progress in Aerospace Sciences 11, 1-66 (1970).
5. C.T. Tran, W. Twomey, R. Dat, Calcul des caractéristiques dynamiques d'une structure d'hélicoptère par la méthode des modes partiels. Rech. Aérospatiale 1973-6, 337-354 (1973).
6. F. Kießling, Anwendung der Standschwingungstechnik bei der Lösung aeroelastischer Probleme von V/STOL-Drehflügelflugzeugen. Presented at the DGLR-Fachausschußsitzung "Drehflügelflugzeuge" in Stuttgart, 18 October 1974 (DLR-Mitt. to appear).
7. K.H. Hohenemser and S.-K. Yin, Some applications of the method of multiblade coordinates. J. American Helicopt. Soc. 17, 3-12 (1972).
8. J.C. Houbolt and G.W. Brooks, Differential equations of motion for combined flapwise bending, chordwise bending, and torsion of twisted nonuniform rotor blades. NACA Report 1346 (1958).

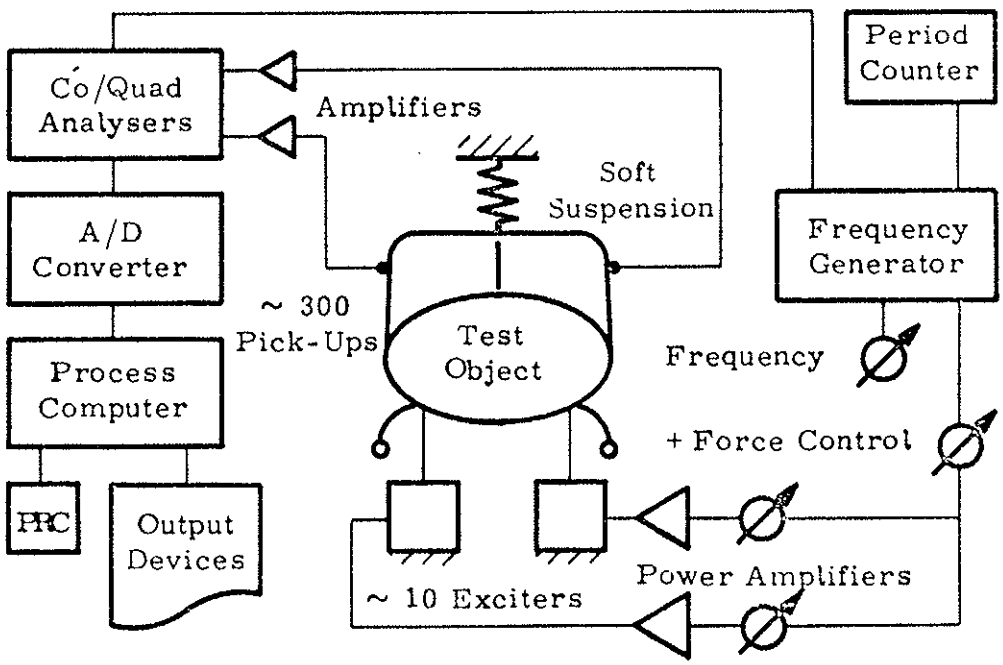

Fig. 1: Schematic Ground Vibration Test Set-Up

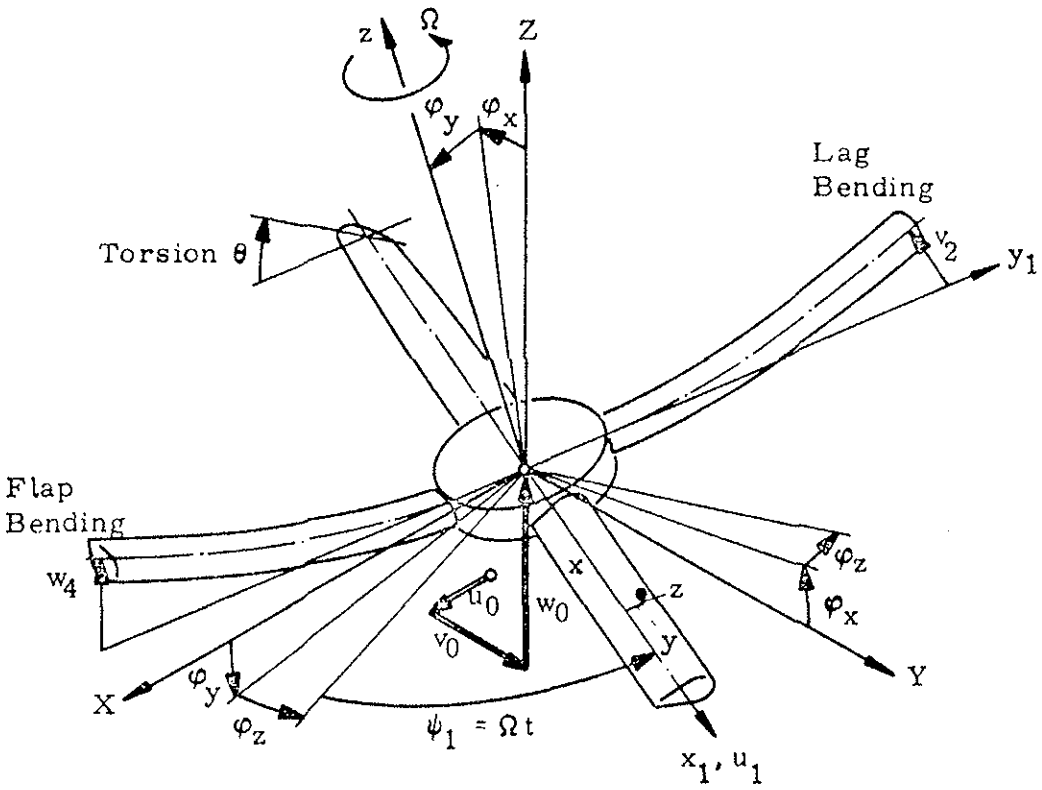

Fig. 2: The Unconstrained Flexible Rotor

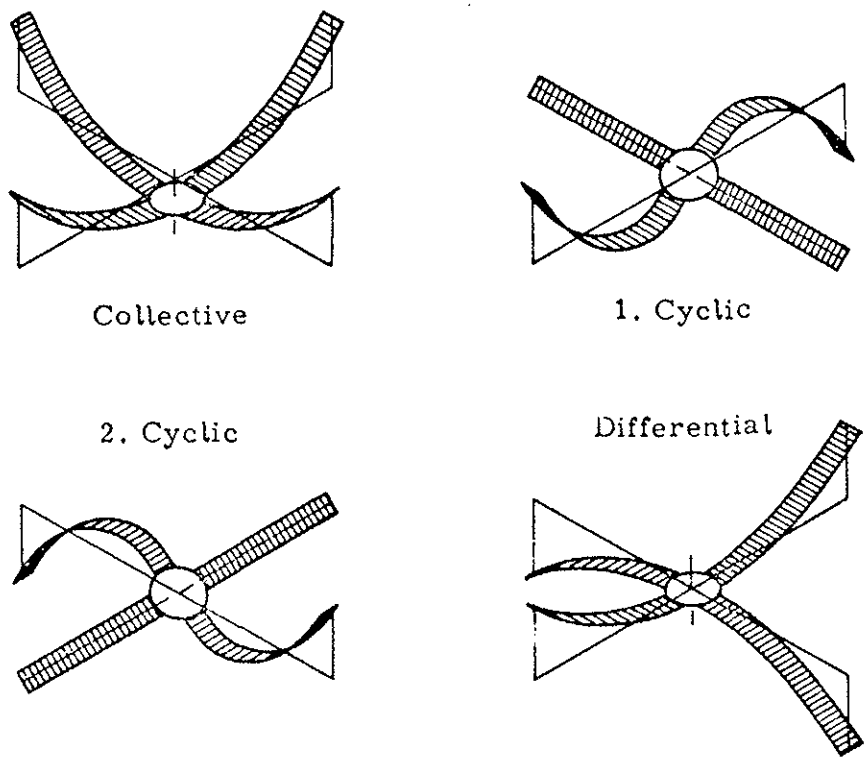

Fig. 3: Typical Unconstrained Rotor Modes

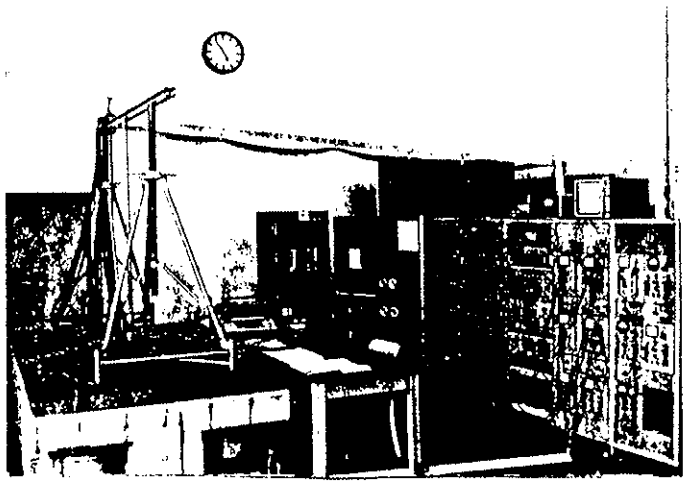

Fig. 4: Rotor model ground vibration test set-up

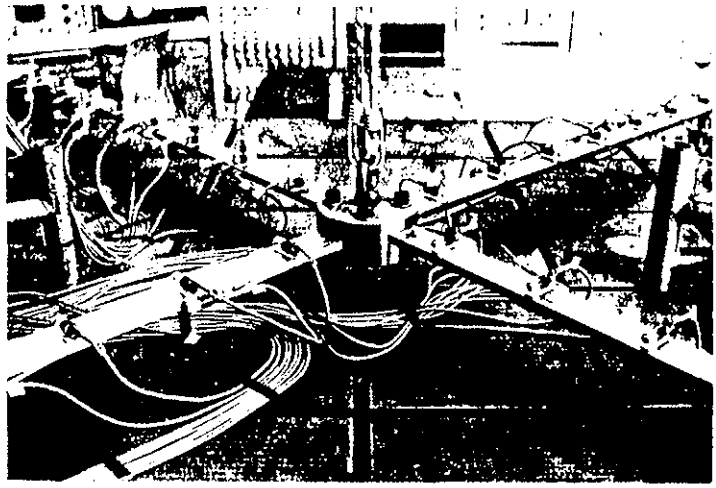

Fig. 5: Hub arrangement and suspension

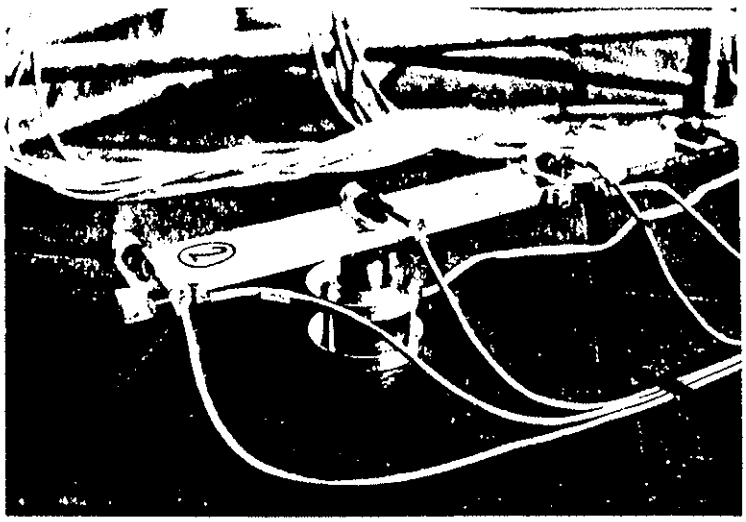

Fig. 6: Acceleration pick-ups and noncontact exciter

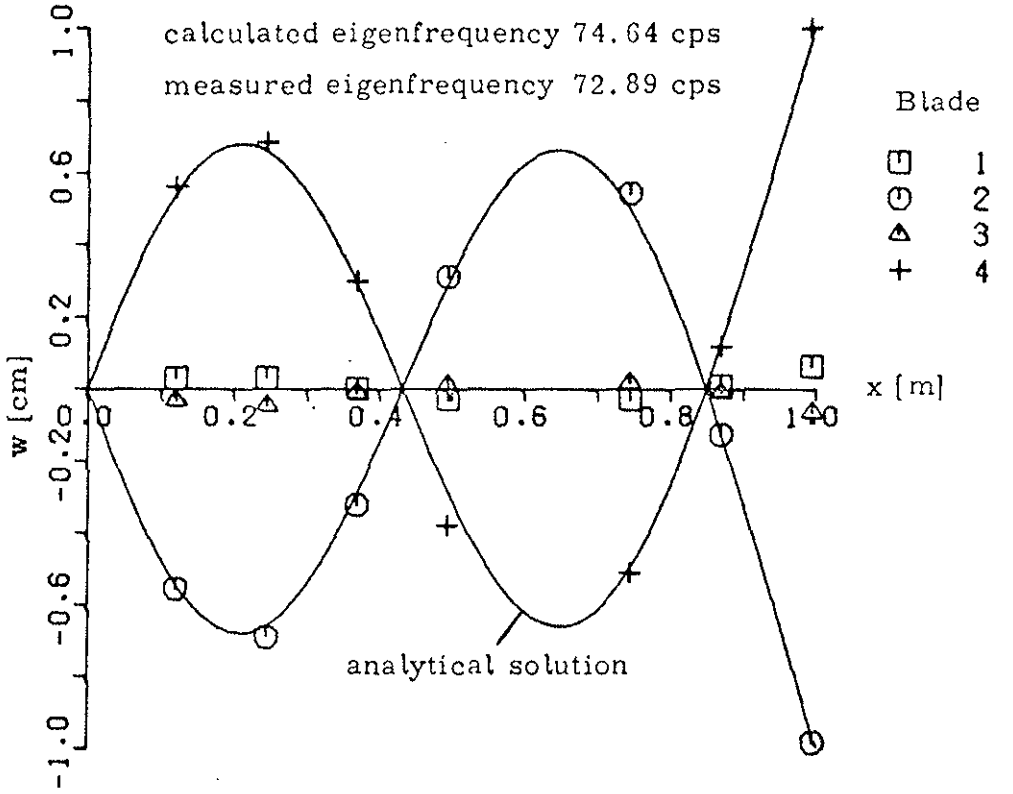

Fig. 7: Example of a rotor mode

Type:		collective			1. antisymmetr.			2. antisymmetr.			differential		
T test A analysis		f_r	M_r	ζ_r	f_r	M_r	ζ_r	f_r	M_r	ζ_r	f_r	M_r	ζ_r
		cps	kgcm²	%	cps	kgcm²	%	cps	kgcm²	%	cps	kgcm²	%
flap	1. T	8.47	3.94	1.03	23.7	2.22	0.35	23.5	2.03	0.48	6.20	3.18	1.38
	1. A	8.41	3.98	--	23.8	1.79	--	23.8	1.79	--	6.18	3.28	--
	2. T	43.7	4.02	0.35	73.8	2.19	0.79	72.9	2.07	0.71	37.9	3.68	0.44
	2. A	45.1	3.82	--	74.6	1.97	--	74.6	1.97	--	38.7	3.28	--
	3. T	114.	3.55	0.76	151.	3.05	0.52	148.	3.16	0.59	106.	4.15	0.42
	3. A	116.	3.57	--	146.	2.40	--	146.	2.40	--	108.	3.28	--
lag	1. T	94.9	3.62	0.47	26.8	1.65	0.72	26.9	1.80	0.70	23.5	3.24	0.84
	1. A	95.8	3.54	--	28.2	1.99	--	28.2	1.99	--	24.7	3.28	--
	2. T	--	--	--	156.	2.96	0.69	155.	3.04	0.79	147.	2.86	0.65
	2. A	--	--	--	163.	1.85	--	163.	1.85	--	155.	3.28	--

Table 1: Model test results in comparison with theoretical analysis

T test A analysis		1. flap		2. flap		3. flap		1. lag		2. lag	
		T	A	T	A	T	A	T	A	T	A
$\Omega/2\pi$ [cps]	0.	6.20	6.18	37.9	38.7	106.	108.	23.5	24.7	147.	155.
	6.18	9.26	9.31	41.0	42.0	109.	112.	23.7	24.9	148.	156.
	12.4	14.9	15.1	49.3	50.7	118.	121.	24.3	25.6	152.	158.
	18.5	21.0	21.4	60.7	62.4	131.	135.	25.1	26.6	157.	161.
	24.7	27.2	27.7	73.8	75.7	147.	153.	26.3	27.9	164.	166.
	30.9	33.5	34.2	87.8	89.9	166.	172.	27.6	29.4	173.	172.

Table 2: Eigenfrequencies of differential modes of the spinning rotor

Appendix

Matrices of the Unconstrained Rotor Equations of Motion

The column of generalized coordinates can be written

$$(A1)\qquad \mathbf{q}_R = \left[u_0\ v_0\ w_0\ \varphi_x\ \varphi_y\ \varphi_z\ \mathbf{q}^{C^T}\ \mathbf{q}^{A^T}\ \mathbf{q}^{B^T}\ \mathbf{q}^{D^T}\right]^T .$$

The mass matrix is diagonal

$$(A2)\qquad \mathbf{M}_R = \lceil M\ M\ M\ I_X\ I_Y\ I_Z\ \mathbf{M}^C\ \mathbf{M}^A\ \mathbf{M}^B\ \mathbf{M}^D \rfloor$$

with elements

$$(A3)\qquad M^C_{rr} = N\int \left(u_r^{c\,2} + v_r^{c\,2} + w_r^{c\,2}\right) dm\,;\quad M^C_{rs} = 0\ \ (r \neq s)\ ,$$

$$(A4)\qquad M^A_{rr} = M^B_{rr} = M^{\alpha}_{rr} = M^{\beta}_{rr} = \frac{N}{2}\int \left(u_r^{a\,2} + u_r^{b\,2} + v_r^{a\,2} + v_r^{b\,2} + w_r^{a\,2} + w_r^{b\,2}\right) dm\,;\quad M^A_{rs} = M^B_{rs} = 0 \quad (r \neq s)$$

$$(A5)\qquad M^D_{rr} = N\int \left(u_r^{d\,2} + v_r^{d\,2} + w_r^{d\,2}\right) dm\,;\quad M^D_{rs} = 0\ \ (r \neq s)\ .$$

The upper triangle of the skew-symmetric gyroscopic matrix reads

$$(A6)\qquad \mathbf{G}_R = \Omega \begin{bmatrix} 0 & & & & & & & & & \\ & 0 & & & & & & & & \\ & & 0 & & & & & & & \\ & & & 0 & I_Z & & \mathbf{G}^{XA} & \mathbf{G}^{XB} & & \\ & & & & 0 & & \mathbf{G}^{YA} & \mathbf{G}^{YB} & & \\ & & & & & 0 & \mathbf{G}^{ZC} & & & \\ & & & & & & \mathbf{G}^{C} & & & \\ & & & & & & & \mathbf{G}^{A} & \mathbf{G}^{AB} & \\ & & & & & & & & \mathbf{G}^{B} & \\ \text{skew-symmetric} & & & & & & & & & \mathbf{G}^{D} \end{bmatrix}$$

with elements

$$(A7)\qquad G^{XA}_r = +G^{YB}_r = -N\int \left(x\, w_r^a + y\, w_r^b\right)\ dm$$

$$(A8)\qquad G^{XB}_r = -G^{YA}_r = -N\int \left(x\, w_r^b - y\, w_r^a\right) dm$$

$$(A9)\qquad G^{ZC}_r = 2N\int \left(x\, u_r^c + y\, v_r^c\right)\ dm$$

$$(A10)\qquad G^{C}_{rs} = -2N\int \left(u_r^c\, v_s^c - v_r^c\, u_s^c\right)\ dm$$

$$(A11)\qquad G^{A}_{rs} = G^{B}_{rs} = -N\int \left(u_r^a\, v_s^a + u_r^b\, v_s^b - v_r^a\, u_s^a - v_r^b\, u_s^b\right)\ dm$$

$$(A12)\qquad G^{AB}_{rs} = 2\,M^A_{rs} + N\int \left(u_r^b\, v_s^a - u_r^a\, v_s^b - v_r^b\, u_s^a + v_r^a\, u_s^b\right) dm$$

$$(A13)\qquad G^{D}_{rs} = -2N\int \left(u_r^d\, v_s^d - v_r^d\, u_s^d\right)\ dm$$

The damping matrix is assumed diagonal

(A14) $$\mathbf{D}_R = \begin{bmatrix} 0 & 0 & 0 & 0 & 0 & 0 & \mathbf{D}^C & \mathbf{D}^A & \mathbf{D}^B & \mathbf{D}^D \end{bmatrix}$$

with elements

(A15) $$D^C_{rs} = 2\,\omega^C_r\,\zeta^C_r\,M^C_{rs}$$

(A16) $$D^A_{rs} = D^B_{rs} = 2\,\omega^A_r\,\zeta^A_r\,M^A_{rs}$$

(A17) $$D^D_{rs} = 2\,\omega^D_r\,\zeta^D_r\,M^D_{rs}$$

The stiffness matrices are all symmetric. The centrifugal terms are included in

(A18) $$\mathbf{K}_C = -\Omega^2 \cdot \begin{bmatrix} 0 & & & & & & & & & \\ & 0 & & & & & & & & \\ & & 0 & & & & & & & \\ & & & 0 & & & & & & \\ & & & & 0 & & & & & \\ & & & & & 0 & & & & \\ & & & & & & \mathbf{K}^C_C & & & \\ & & & & & & & \mathbf{K}^A_C & \mathbf{K}^{AB}_C & \\ & & & & & & & & \mathbf{K}^B_C & \\ & & & & & & \text{symmetric} & & & \mathbf{K}^D_C \end{bmatrix}$$

with elements

(A20) $$K^C_{Crs} = M^C_{rs} - N\int w^c_r\, w^c_s\, dm\ ,$$

(A21) $$K^A_{Crs} = K^B_{Crs} = 2M^A_{rs} - \frac{N}{2}\int \left[(w^a_r w^a_s + w^b_r w^b_s) - 2(v^a_s u^b_r + v^a_r u^b_s - u^a_s v^b_r - u^a_r v^b_s) \right] dm$$

(A22) $$K^{AB}_{Crs} = 2M^B_{rs} - \frac{N}{2}\int \left[(w^a_r w^b_s - w^b_r w^a_s) - 2(u^a_r v^a_s - v^a_r u^a_s - u^b_s v^b_r + v^b_s u^b_r) \right] dm\ ,$$

(A23) $$K^D_{Crs} = M^D_{rs} - N\int w^d_r\, w^d_s\, dm\ .$$

The geometric stiffness reads

(A24) $$\mathbf{K}_G = -\Omega^2 \cdot \begin{bmatrix} 0 & & & & & & & & & \\ & 0 & & & & & & & & \\ & & 0 & & & & & & & \\ & & & 0 & & & & & & \\ & & & & 0 & & & & & \\ & & & & & 0 & & & & \\ & & & & & & \mathbf{K}^C_G & & & \\ & & & & & & & \mathbf{K}^A_G & \mathbf{K}^{AB}_G & \\ & & & & & & & & \mathbf{K}^B_G & \\ & & & & & & \text{symmetric} & & & \mathbf{K}^D_G \end{bmatrix}$$

with elements

(A25) $$K^C_{Grs} = N\int \left[x\left(u^{cc}_{rs} + u^{cc}_{sr}\right) + y\left(v^{cc}_{rs} + v^{cc}_{sr}\right) \right] dm$$

(A26) $$K^A_{Grs} = K^B_{Grs} = \frac{N}{2}\int \left[x(u^{aa}_{rs} + u^{bb}_{rs} + u^{aa}_{sr} + u^{bb}_{sr}) + y(v^{aa}_{rs} + v^{bb}_{rs} + v^{aa}_{sr} + v^{bb}_{sr}) \right] dm$$

(A27) $$K^{AB}_{Grs} = \frac{N}{2}\int \left[x(u^{ab}_{rs} - u^{ba}_{rs} + u^{ba}_{sr} - u^{ab}_{sr}) + y(v^{ab}_{rs} - v^{ba}_{rs} + v^{ba}_{sr} - v^{ab}_{sr}) \right] dm$$

(A28) $K^{D}_{Grs} = N\int \left[x(u^{dd}_{rs} + u^{dd}_{sr}) + y(v^{dd}_{rs} + v^{dd}_{sr}) \right] dm$

The u^{ab}_{rs}, for example, is a second order displacement which can be computed using equation (25) by inserting the values of a (r, a)-mode and a (s, b)-mode as factors.

The elastic stiffness matrix is diagonal

(A29) $\mathbf{K}_E = \left[0\ 0\ 0\ 0\ 0\ 0\ \mathbf{K}^{C}_{E}\ \mathbf{K}^{A}_{E}\ \mathbf{K}^{B}_{E}\ \mathbf{K}^{D}_{E} \right]$

with elements

(A30) $K^{C}_{Ers} = \omega^{C^2}_{r} M^{C}_{rs}$,

(A31) $K^{A}_{Ers} = K^{B}_{Ers} = \omega^{A^2}_{r} M^{A}_{rs}$,

(A32) $K^{D}_{Ers} = \omega^{D^2}_{r} M^{D}_{rs}$.

The transformation (17) yield a skew-symmetric matrix

$$\mathbf{E}_R = \Omega \cdot \begin{bmatrix} 0 & & & & & & & & & \\ & 0 & & & & & & & & \\ & & 0 & & & & & & & \\ & & & 0 & & & & & & \\ & & & & 0 & & & & & \\ & & & & & 0 & & & & \\ & & & & & & \mathbf{O} & & & \\ & & & & & & & \mathbf{O} & \mathbf{E}^{AB} & \\ & & & & & & & & \mathbf{O} & \\ & & & & & & & & & \mathbf{O} \end{bmatrix}$$

skew-symmetric

with

(A34) $E^{AB}_{rs} = 2D^{A}_{rs}$

which depends on damping.

Finally, the generalized forces read

(A35) $\mathbf{Q}_R = \left[F_X\ F_Y\ F_Z\ M_X\ M_Y\ M_Z\ \mathbf{Q}^{C^T}\ \mathbf{Q}^{A^T}\ \mathbf{Q}^{B^T}\ \mathbf{O} \right]^T$

with elements

(A36) $Q^{C}_{r} = F_Z\, w^{c}_{rH} + M_Z\, \varphi^{c}_{zrH} + N\Omega^2 \int (x\, u^{c}_{r} + y\, v^{c}_{r})\ dm$

(A37) $Q^{A}_{r} = 2\left(F_X\, u^{a}_{rH} + F_Y\, v^{a}_{rH} + M_X\, \varphi^{a}_{xrH} + M_Y\, \varphi^{a}_{yrH} \right)$

(A38) $Q^{B}_{r} = 2\left(F_X\, u^{b}_{rH} + F_Y\, v^{b}_{rH} + M_X\, \varphi^{b}_{xrH} + M_Y\, \varphi^{b}_{yrH} \right)$